# Interface induced giant magnetoelectric coupling in multiferroic superlattices

Hongwei Wang and Lixin He*
*Key Laboratory of Quantum Information, University of Science and Technology of China, Hefei, Anhui, 230026, People's Republic of China*

Xifan Wu†
*Department of Physics and Institute for Computational Molecular Science Temple University, Philadelphia, PA 19122, USA*
(Dated: December 4, 2018)

The electric and magnetic properties of $(BaTiO_3)_n/(CaMnO_3)_n$ short-period superlattices are studied by the first-principles calculations. The local electric polarizations in the $CaMnO_3$ layers are significant, comparable to that in the $BaTiO_3$ layers. Remarkably, the electric polarization is almost doubled when the spin configuration changes from antiferromagnetic to ferromagnetic in the superlattices, indicating a giant magnetoelectric coupling. This enhancement of the magnetoelectric coupling is due to the suppression of the antiferrodistortive mode in the $CaMnO_3$ layers at the interfaces.

PACS numbers: 77.22.-d, 77.22.Ej, 77.80.-e, 77.84.Lf



The emergence of new phenomena at artificial heterostructure is currently at the center of scientific and technological interest [1–5]. Because a large variety of degrees of freedom such as spin, charge, structural orderings can be found in $ABO_3$ perovskite, it presents an ideal playground to explore the interactions among various orderings that could potentially lead to enhanced functionalities, and multifunctional materials [1, 5].

Multiferroics are among these multifunctional materials that have attracted intensive interests recently [6]. The ferroelectric/(anti)-ferromagnetic superlattices (SLs) may have strong electric polarization, magnetic ordering and magnetoelectric coupling simultaneously which is rarely seen in single phase bulk materials because of the symmetry restrictions [7]. Conventionally, the magnetoelectric coupling can be introduced by the mechanical boundary condition through the in-plane strain or the electric boundary condition through charge continuity satisfied by the constituent materials [7]. However, the interfaces separating different constituent materials can carry distinct instabilities originated from individual parent bulk materials [1]. We show that the interfacial competition of instabilities [8] may lead to surprisingly enhancement of the magnetoelectric coupling, which arising from the interfacial atomistic effects, can be much larger than that through the continuum media coupling.

$AMnO_3$ (A=Ca, Sr, ...) are good candidates as building blocks for the multiferroic supperlattices, because they have several competing instabilities [9] coupled to the magnetic ordering. In $AMnO_3$, Mn atom has partially occupied *d*-orbitals, and the Mn-O-Mn bond angle is crucial in controlling the magnetic interactions, which at the same time also strongly couples to the oxygen octahedral rotation (AFD) and ferroelectric (FE) soft mode. The coupling between the spin, the AFD modes and the FE modes depends on the relative energetics of these instabilities. Unfortunately in bulk $AMnO_3$, there is a strong AFD instability associated with a large oxygen octahedral rotation that suppresses the FE mode[9]. As a result, the *linear* magnetoelectric (spin-ferroelectricity) coupling is usually found to be weak.

In this letter, we demonstrate, through first-principles calculations, that the energetics of the AFD, FE and magnetic ordering can be drastically modified [10] by interface engineering to favorite the magnetoelectric coupling. We take the $CaMnO_3$(CMO)/$BaTiO_3$(BTO) SLs as our model systems. We find that the $MnO_6$ octahedral rotation will be strongly suppressed by the neighboring BaO layers, leading to the enormous enhancement of magnetoelectric coupling as well as FE at interfaces. This enhancement will be strengthened with the increasing density of interfaces and reaches its maximum at the shortest SL, (i.e., $n$=1) where one observes a huge change of electric polarization between the antiferromagnetic (AFM) and ferromagnetic (FM) states. To better clarify the mechanism for its underlying physics, an effective Hamiltonian model is also developed. The model explicitly shows that an increased magnetoelectric coupling develops with a completely suppressed AFD, which consistently explains our computational results.

The calculations are based on the standard density functional (DFT) theory with spin-polarized generalized gradient approximation, implemented in the Vienna ab initio simulations package (VASP) [11, 12]. We adopt the Perdew-Burke-Ernzerhof functional revised for solids (PBEsol)[13]. The on-site Coulomb $U$=4.0 eV and exchange interaction $J$ =0.88 eV are used for the Mn 3d electrons [14]. We use the plane-wave basis and projector augmented-wave pseudopotentials [15]. A 500 eV energy cutoff and 6×6×2 k-point meshes converge the results very well. All ionic coordinates are fully relaxed until the Hellman-Feynman forces on the ions are less than 1 meV/Å. The electric polarizations are computed using

the Berry phase theory of polarization [16].

The calculated lattice constants of cubic $CaMnO_3$ and $BaTiO_3$ are 3.731Å and 3.987Å respectively using PBEsol functional [13], compared with the experimental values 3.73Å and 3.993Å, which are much more accurate than the those obtained from LDA. This is very important for studying ferroelectrics, whose properties are very sensitive to the lattice constants.

The ground state of orthorhombic (bulk) $CaMnO_3$ is G-type antiferromagnetic. We find a small FE instability related to an unstable polar mode in the high symmetry cubic phase, with an imaginary frequency $\omega_{FE}$=3.43$i$ cm$^{-1}$ and a much larger antiferro-distortive (AFD) instability associated to a nonpolar oxygen rotational mode with an imaginary frequency $\omega_{AFD}$=219$i$ cm$^{-1}$, consistent with previous calculations[9]. As a result, the octahedra rotate a angle about 8.94°. In contrast, BaTiO3 is highly resistant to oxygen octahedral rotations and exhibits a robust FE state at room temperature.

The lattice mismatch between CMO and BTO is about 6.59%, which might be too large to grow high quality CMO/BTO SLs. One may grow the CMO/BTO SLs on the $NdGaO_3$ substrate to reduce the lattice mismatch between CMO and BTO to about 3.37%. We therefore fix the in-plane lattice constants of the SL to those of $NdGaO_3$ substrates (3.86 Å) in the calculations. We have studied two short-period SLs structures $(BaTiO_3)_1/(CaMnO_3)_1$ (1:1) and $(BaTiO_3)_2/(CaMnO_3)_2$ (2:2). In the calculations, we fix the symmetry of the SLs to the space group P4bm, allowing the $MnO_6$ and $TiO_6$ octahedra to rotate. We neglect the tilting of $MnO_6$ octahedra (rotations about an in-plane axis), because oxygen tilting requires a coherent pattern of tilts that would propagate into the BTO unit cells, where octahedral rotations are unfavorable.

To determine the ground-state spin structure, we calculate the total energies of a set of spin configurations (SCs) for the 1:1 and 2:2 SLs with full relaxations of the (electronic and lattice) structures. The results show that the stablest SCs are G-type AFM for 1:1, and A-type AFM for 2:2 SLs. The calculated magnetic moments of Mn ions are about 2.9 $\mu_B$, whereas Ti ions have negligible induced magnetic moments. We further fit the exchange integrals to a Heisenberg model $H = 1/2 \sum_{i,j} J_{ij} \mathbf{S}_i \cdot \mathbf{S}_j$, assuming nearest neighbor coupling between the Mn ions. In the 1:1 SL, the intra-layer exchange interaction $J_{\rm intra}$ = -4.8 meV/$\mu_B^2$, and the inter-layer exchange interaction $J_{\rm inter}$ = -0.86 meV/$\mu_B^2$. In the 2:2 SL, the exchange interaction in the $MnO_2$ layer that sandwiched by the two CaO layer $J^{(1)}_{\rm intra}$ = 8.61 meV/$\mu_B^2$, and in the $MnO_2$ layer that adjacent to the BaO layer $J^{(2)}_{\rm intra}$ = -1.11 meV/$\mu_B^2$. The interlayer exchange interaction $J^{(1)}_{\rm inter}$ = -24.54 meV/$\mu_B^2$ and $J^{(2)}_{\rm inter}$ =-0.04 meV/$\mu_B^2$ respectively. Here, the magnetic moments $\mathbf{S}$ are normalized to 1. The $J^{(2)}_{\rm intra}$ in the 2:2 SL is slightly frustrated. The Néel temperatures of the 1:1 and 2:2 SLs are 52 K and 59 K respectively calculated from Monte Carlo simulations [17]. This is because the Néel temperature of bulk CMO is low ($\sim$ 130 K) [18]. The Néel temperature of the SLs can be enhanced by using other $AMnO_3$ compounds with higher Néel temperatures.

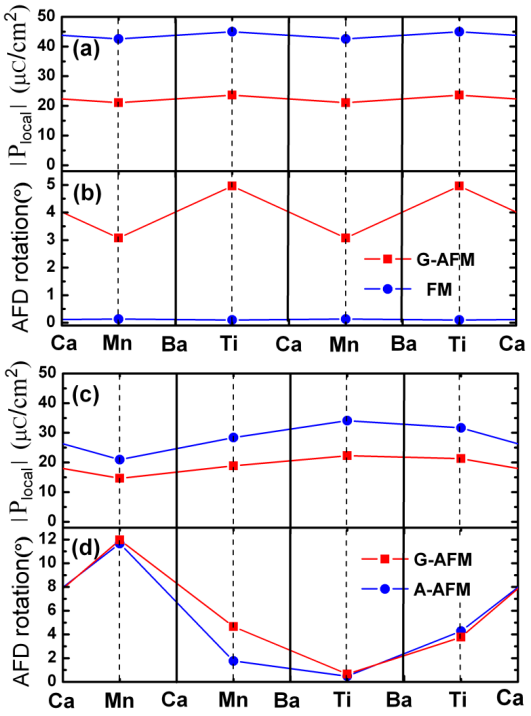


FIG. 1: (Color oline) (a) The local electric polarizations and (b) the AFD rotations of the $MnO_2$ and $TiO_2$ layers in the 1:1 SL of the G-type AFM (red line) and FM states (blue line). (c) The local electric polarizations and (d) the AFD rotations of the $MnO_2$ and $TiO_2$ layers in the 2:2 SL of the G-type AFM (red line) and A-type AFM states (blue line).

Figure 1 (b), (d), depict the local AFD associated with the $TiO_6$ or $MnO_6$ octahedral rotation in 1:1 and 2:2 SLs respectively. Clearly, the $MnO_6$ octahedral that sandwiched between two CaO layers in 2:2 SL keeps a large rotation angle around 12° and $TiO_6$ octahedra that sandwiched between two BaO layers has a rotation almost around 0°. This is in consistent with the fact that CMO bulk has a strong AFD instability and BTO strongly resists the octahedra rotation. What is more intriguing, however, is the behavior of the interfacial layers of $MnO_6$ octahedra. Because of the presence of BaO on one side and CaO on the other side, $MnO_6$ at interface is exposed to a strongly broken mirror symmetry. As a result, this $MnO_6$ octahedra is found to have significantly reduced rotation angle which is around 4.6° and 3.0° in 2:2 and 1:1 SL respectively.

In bulk $CaMnO_3$, it is the strong AFD that suppresses the FE instability from condensation at ground states. Because of the greatly reduced interfacial $MnO_6$ octa-

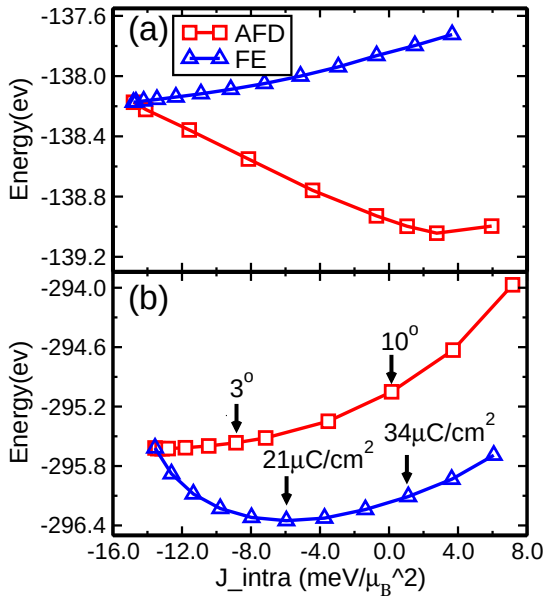


FIG. 2: (Color oline) The total energies as functions of the $MnO_2$ intra-layer exchange energy $J_{\rm intra}$ for (a) bulk $CaMnO_3$ and (b) 1:1 SL through AFD rotation and FE modes. We also show the AFD rotation angle, and the polarization of the FE mode in the 1:1 SL.

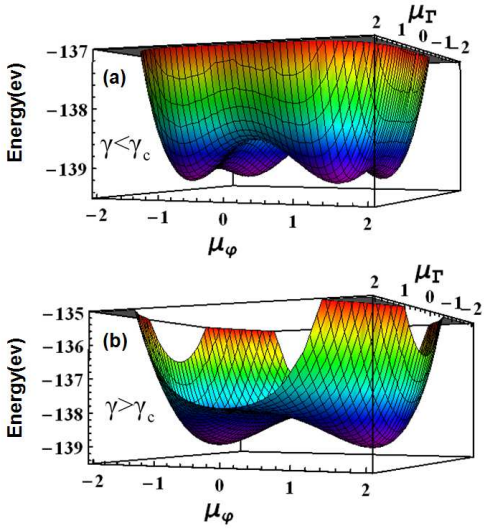


FIG. 3: Schematic shows of the energy surfaces of the effective Hamiltonian Eq. 1, in the case of (a) the coupling coefficient $\gamma < \gamma_c$, and (b) the coupling coefficient $\gamma > \gamma_c$, when both $\alpha$ <0, and $\beta$ <0.

hedra rotation, together with strong polarization in the $BaTiO_3$ layers, one might expect that the FE can develop in the $CaMnO_3$ layer of the SL. Indeed, we find that both 1:1 and 2:2 SLs become multiferroic with spontaneous polarizations of 21.30 $\mu$C/cm$^2$ and 27.52 $\mu$C/cm$^2$ respectively computed by Berry phase formalism. To gain more insight, we calculate the layer polarization along [001] direction $p_z = \sum_i (e/\Omega) Z_i^* \lambda_i$ based on the linear approximation involving effective charges $Z_i^*$ and small ionic distortions $\lambda_i$ of each atoms $i$ in the cell from a higher central symmetric nonpolar reference structure. The effective charges are obtained from the cubic $CaMnO_3$ and $BaTiO_3$ phase by finite difference method. The resulting layer polarizations are presented in Fig.1. It can be seen that $MnO_2$ centered layers becomes polarized to almost the same degree of $TiO_2$-centered layers in both 1:1 and 2:2 SLs.

The development of multiferroic behavior in the $CaMnO_3$ component in the sperlattices has now been established. It provides us an opportunity to study the magnetoelectric coupling directly. To this end, we compare the electric polarizations under various spin configurations. As one of the most interesting results, we find that the electric polarization undergoes a huge increase from about 21 $\mu$C/cm$^2$ to about 38 $\mu$C/cm$^2$ in 1:1 SL when the $MnO_2$ intra-layer spin configuration is changed from antiferromatic ($C$-type or $G$-type AFM) to ferromagnetic (FM or $A$-AFM). In 2:2 SL, we observe a similar however weaker enhancement of polarization from about 19 $\mu$C/cm$^2$ to about 30 $\mu$C/cm$^2$. The above result indicates that the magnetoelectric coupling is giant!

At a closer inspection of what happen locally in the SLs, the above drastic polarization change is also found to be accompanied by a almost homogeneous increased layer polarization for both $MnO_2$-centered and $TiO_2$-centered layers in both 1:1 and 2:2 SLs and a further drop of the interfacial $MnO_6$ octhedra rotations.

It is well known that the Mn-O-Mn exchange angle is essential in controlling the magnetic ordering [19]. In multiferroics where spin, FE and AFD instabilities are all present, Mn-O-Mn angle can be strongly coupled to $MnO_6$ octahedral rotation and FE soft phonon modes. In Fig. 2(a), (b), we present the change of the total energy as a function of the intra-layer exchange integral $J_{\rm intra}$ in bulk CMO and 1:1 SL respectively. It can be seen that intra-layer spin ordering can be continuously tuned from AFM($J_{\rm intra} < 0$) to FM($J_{\rm intra} > 0$) by increasing either the $MnO_6$ octahedral rotation (red) or the amplitude of the FE soft phonon mode in both bulk $CaMnO_3$ and 1:1 SL. In bulk CMO, the intra-layer AFM-FM phase transition is realized by the increased octahedral rotation which has a much lower total energy than that of increased FE soft phonon mode. However in 1:1 SLs, the $MnO_6$ octahedral rotation is lagerly suppressed by the interface because it becomes energetically unfavorable [see Fig. 2(b)]. Thus, AFM-FM phase transition can be only driven by the increased FE soft phonon mode which results in the observed enhanced magnetoferroelectric coupling.

It is clear that the enhancement of the magnetoelectric coupling originates from the interface where the relative energetics of spin, FE and AFD are changed compared with bulk $CaMnO_3$. The AFD instability is largely suppressed thus the spin-polarization coupling strength is in-

creased. To further understand how the interface tunes the competetion between the AFD and FE modes, we resort to an effective Hamiltonian. For bulk $CaMnO_3$ in a uniform phase, the effective Hamiltonian is,

$$E(\{\mathbf{u}_\Gamma, \mathbf{u}_\varphi\}) = E_0 - \sum_{ij} J_{ij}(0)\mathbf{S}_i \cdot \mathbf{S}_j + \alpha\mathbf{u}_\Gamma^2 + \beta\mathbf{u}_\varphi^2 + \eta\mathbf{u}_\Gamma^4 + \kappa\mathbf{u}_\varphi^4 + \gamma\mathbf{u}_\Gamma^2\mathbf{u}_\varphi^2 , \quad (1)$$

where, $\mathbf{u}_\Gamma$ and $\mathbf{u}_\varphi$ are the FE and AFD modes respectively. The phonon frequencies $\alpha = \frac{1}{2}m_\Gamma\omega_\Gamma^2 - \sum_{ij}\frac{\partial^2 J_{ij}}{\partial^2 u_\Gamma}\mathbf{S}_i \cdot \mathbf{S}_j$ and $\beta = \frac{1}{2}m_\varphi\omega_\varphi^2 - \sum_{ij}\frac{\partial^2 J_{ij}}{\partial^2 u_\varphi}\mathbf{S}_i \cdot \mathbf{S}_j$ strongly depend on the spin configurations of the system. The anharmonic terms $\kappa$, $\eta$ are positive. $\gamma$ which describes the coupling between the FE and AFD modes, is also positive. At the energy minima, we have $\partial E(\{\mathbf{u}_\Gamma, \mathbf{u}_\varphi)/\partial\mathbf{u}_\Gamma$=0, and $\partial E(\{\mathbf{u}_\Gamma, \mathbf{u}_\varphi)/\partial\mathbf{u}_\varphi$=0, i.e.,

$$\alpha\mathbf{u}_\Gamma + 2\eta\mathbf{u}_\Gamma^3 + \gamma\mathbf{u}_\Gamma\mathbf{u}_\varphi^2 = 0 \quad (2)$$

$$\beta\mathbf{u}_\varphi + 2\kappa\mathbf{u}_\varphi^3 + \gamma\mathbf{u}_\varphi\mathbf{u}_\Gamma^2 = 0 \quad (3)$$

It is easy to see from the equations that if $\alpha > 0$ ($\beta > 0$), we have $\mathbf{u}_\Gamma$=0 ($\mathbf{u}_\varphi$=0). The interesting cases are that both $\alpha$ and $\beta$ are negative. When the coupling between the two modes is weak, i.e., $\gamma < \gamma_c = \min(2\kappa\alpha/\beta, 2\eta\beta/\alpha)$, one has a solution that both $\mathbf{u}_\Gamma$ and $\mathbf{u}_\varphi$ are non-zero as schmeatically shown in Fig. 3 (a). However, when $\gamma > \gamma_c$, one has $\mathbf{u}_\Gamma$=0 and $\mathbf{u}_\varphi^2 = -\beta/2\kappa$, if $\beta/2\kappa < \alpha/2\eta$, ($\mathbf{u}_\varphi$=0 and $\mathbf{u}_\Gamma^2 = -\alpha/2\eta$, if $\beta/2\kappa > \alpha/2\eta$), i.e., one of the soft mode is fully suppressed by the other mode that has stronger instability, because of the coupling between the two modes, as shown in Fig. 3 (b). This is exactly the case in $CaMnO_3$. In bulk materials, the AFD mode is more unstable, therefore the FE mode is fully suppressed. In the 1:1 SL, when the $MnO_2$ intra-layer spin configuration is AFM, the AFD instability $\alpha$ is still larger than that of the FE mode despite of the interface effects, therefore, there are still significant AFD rotations, even though they are smaller than those in bulk CMO. However, when the $MnO_2$ intra-layer spin configuration changes to FM, the FE instability is enhanced [20], and becomes stronger than the AFD instability with the help of the BaO layer pinning effects to the AFD mode. Therefore, the AFD mode is fully suppressed. The suppression of the AFD mode greatly enhances the FE modes, again because of the coupling between the FE and AFD modes. The results for the 2:2 SL can also be understood in the same scenario.

The magnetoelectric coupling effects in the CMO/BTO SLs can be observed by various experimental techniques. For example, one should be able to observe large polarization change by applying magnetic field. This can be best seen near the paramagnetic (PM) to AFM phase transition temperatures, where relative small magnetic field is needed. Or one may simply observe the polarization change at PM to AFM transitions. Beside the electric polarization, the dielectric constants are also expected to change dramatically under magnetic field near the magnetic phase transitions.

To summarize, we have demonstrated a novel mechanism that could lead to giant magnetoferroelectric coupling in the multiferroic $CMnO_3/BaTiO_3$ superlattices. The key idea is that the energetics of the instabilities, such as antiferro-distortive mode, ferroelectric mode, and the magnetic ordering can be drastically modified by interface engineering to enhance the magnetoelectric coupling. The enhancement of the magnetoelectric coupling is due to the interface atomistic effects which could be much stronger than those with mechanical coupling. It therefore opens a new path to design novel multiferroic superlattices with strong magnetoelectric coupling.

We acknowledge X. X. Xi for useful discussions. LH acknowledges the support from the Chinese National Fundamental Research Program 2011CB921200 and National Natural Science Funds for Distinguished Young Scholars. XW acknowledges the support by the National Science Foundation through TeraGrid resources provided by NICS under grant number [TG-DMR100121].

* Electronic address: helx@ustc.edu.cn
† Electronic address: xifanwu@temple.edu

[1] E. Bousquet, M. Dawber, N. Stucki, C. Lichtensteiger, P. Hermet, S. Gariglio, J. M. Triscone, and P. Ghosez, Nature **452**, 06817 (2008).
[2] H. N. Lee, H. M. Christen, M. F. Chisholm, C. M. Rouleau, and D. H. Lowndes, Nature **433**, 395 (2005).
[3] A. Ohtomo and H. Y. Huang, Nature **427**, 423 (2004).
[4] P. Yu, J. S. Lee, S. Okamoto, M. D. Rossell, M. Huijben, C.-H. Yang, Q. He, J. X. Zhang, S. Y. Yang1, M. J. Lee, et al., Phys. Rev. Lett. **105**, 027201 (2010).
[5] J. M. Rondinelli, M. Stengel, and N. A. Spaldin, Nature. Nanotechnology **3**, 46 (2008).
[6] N. A. Spaldin, S. W. Cheong, and R. Ramesh, Physics Today. **63**, 38 (2010).
[7] M. Fiebig, J. Phys. D: Appl. Phys. **38**, R123 (2005).
[8] D. I. Bilc and D. J. Singh, Phys. Rev. Lett. **96**, 147602 (2006).
[9] S. Bhattacharjee, E. Bousquet, and P. Ghosez, Phys. Rev. Lett. **102**, 117602 (2009).
[10] X. F. Wu, , K. M. Rabe, and D. Vanderbilt, Phys. Rev. B **83**, 020104R (2011).
[11] G. Kresse and J. Hafner, Phys. Rev. B **47**, R558 (1993).
[12] G. Kresse and J. Furthmuller, Phys. Rev. B **54**, 11169 (1996).
[13] J. P. Perdew, A. Ruzsinszky, G. I. Csonka, O. A. Vydrov, G. E. Scuseria, L. A. Constantin, X. L. Zhou, and K. Burke, Phys. Rev. Lett. **100**, 136406 (2008).
[14] A. I. Liechtenstein, V. I. Anisimov, and J. Zaanen, Phys. Rev. B **52**, 5467 (1995).
[15] P. E. Blochl, Phys. Rev. B **50**, 17953 (1994).
[16] R. D. King-Smith and D. Vanderbilt, Phys. Rev. B **47**, 1651 (1993).
[17] K. Cao, G.-C. Guo, D. Vanderbilt, and L. He, Phys. Rev.

Lett. **103**, 257201 (2009).
[18] E. O. Wollan and W. C. Koehler, Phys. Rev. **100**, 545 (1955).
[19] K. Yamauchi, F. Freimuth, S. Blügel, and S. Picozzi, Phys. Rev. B **78**, 014403 (2008).
[20] J. H. Lee and K. M. Rabe, Phys. Rev. Lett. **104**, 207204 (2010).